

NEW UNDULATOR AND FRONT END FOR XAIRA BEAMLINE AT ALBA

J. Campmany[†], J. Marcos, V. Massana, ALBA-CELLS, Barcelona, Catalonia, Spain

Abstract

A new microfocus beamline for macromolecular crystallography, XAIRA, is being built at ALBA synchrotron light source. The light source for this new beamline is an in-vacuum undulator that can reach the spectral range from 4 keV up to 20 keV. The in-vacuum undulator was tendered in 2018 and awarded to Kyma-RI consortium, and will be delivered to ALBA in November 2019. The Front End has been designed accordingly. It was tendered in 2018 and awarded to FMB. It will be delivered in October 2019. In this paper we present the ID and FE designs.

SCIENTIFIC CASE

ALBA synchrotron light facility currently hosts eight operating beamlines, including one dedicated to Macromolecular Crystallography (MX), BL13-XALOC. Current expansion plans include a specific microfocus MX beamline, XAIRA [1].

XAIRA aims at providing a full beam with a size of $3 \times 1 \mu\text{m}^2$ FWHM ($h \times v$) and a flux of $>3 \times 10^{12}$ ph/s (250 mA in Storage Ring) at 1 Å wavelength (12.4 keV) to tackle MX projects for which only tiny ($<10 \mu\text{m}$) or imperfect crystals are obtained. Besides, XAIRA aims at providing photons at low energies down to 4 keV to support MX experiments exploiting the anomalous signal of the metals naturally occurring in proteins (native phasing), which is enhanced in the case of small crystals and long wavelengths.

UNDULATOR REQUIREMENTS

In order to fulfill the scientific requirements, a hybrid, in-vacuum and long undulator has been designed, with parameters detailed in Table 1.

Table 1: Main Parameters of XAIRA Undulator

Undulator type	In-vacuum
Magnetic configuration	Planar hybrid
Magnetic material	NdFeB
Pole material	Permendur
Period length	19.9 ± 0.02 mm
Number of periods	115
Maximum magnetic length	2.3 m
Magnetic minimum gap	5.2 mm
Minimum physical gap	4.8 mm
Gap range (magnetic)	5.2 mm to 30 mm
Min. effective K at min. gap	2.1085

[†] campmany@cells.es

ID DESIGN

Block and Pole Designs

Blocks are box-type with chamfers in edges allowing clamp fixations and longitudinal chamfers to prevent demagnetization. Mechanical tolerances have been assumed to give changes in the peak field smaller than 0.1%. Selected magnetic material is NdFeB with remanence $B_r = 1.34$ T and coercivity $\mu_0 H_{cJ} \geq 1.5$ T. Poles will be made of high permeability Vanadium Permendur. The optimization of central pole in this case leads to the block and pole dimensions specified in Tables 2 and 3. Shapes are shown in Fig. 1. The undulator central part is shown in Fig. 2

Table 2: Magnetic Block Characteristics

Width	60.0 ± 0.05 mm
Height	40.0 ± 0.05 mm
Length	7.164 ± 0.02 mm
Transverse chamfer angle	45.00°
Transverse chamfer side	4.0 ± 0.02 mm
Longitudinal chamfer angle	45.00°
Longitudinal chamfer side	1.00 ± 0.02 mm
Remanent field	1.34 T
Permeability on axis	1.06
Transversal axis permeability	1.17

Table 3: Iron Pole Characteristics

Width	40.0 ± 0.05 mm
Height	40.0 ± 0.05 mm
Length	2.786 ± 0.02 mm
Transverse chamfer angle	45.00°
Transverse chamfer side	4.0 ± 0.02 mm
Longitudinal chamfer angle	45.00°
Ear width	4.0 ± 0.1 mm
Ear height	3.0 ± 0.1 mm

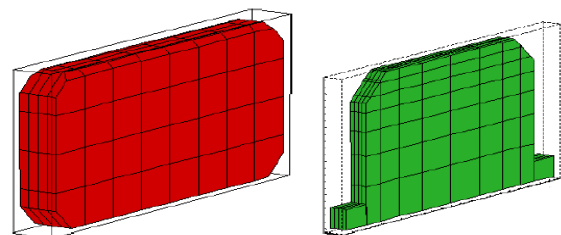


Figure 1: Shapes of blocks (red) and poles (green) in the hybrid design.

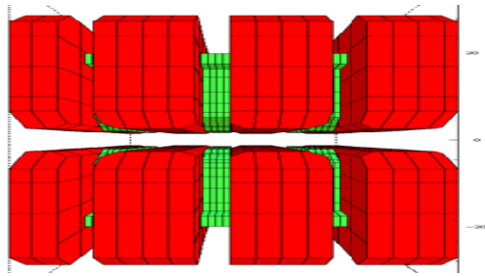


Figure 2: Arrangement of poles and blocks.

Undulator Design

We modelled the whole undulator using RADIA.[2] The magnetic field, first and second field integrals are shown in Figs. 3 to 5 for a gap of 5.2 mm. The orbit is offset by $-75.35 \text{ T}\cdot\text{mm}^2$ corresponding to $-7.53 \mu\text{m}$ for a 3 GeV electron beam. Poles have been optimized to obtain a good field region for $|x| \leq 10 \text{ mm}$ in which the field is uniform within 0.3%. Maximum field on axis is 1.2275 T. The main characteristics of the magnetic field generated by the undulator are summarized in Table 4.

Table 4: Undulator Characteristics

Harmonic analysis	
Undulator period	19.9 mm
Undulator magnetic gap	5.2 mm
Undulator symmetry	symmetric
Peak field	1.2275 T
Effective field	1.1472 T
Effective K	2.1323
High order contribution	6.5%
Fundamental	1.1469 T
3 rd harmonic	0.0775 T
5 th harmonic	0.0030 T
7 th harmonic	0.0002 T

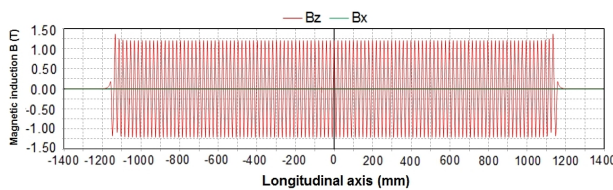


Figure 3: Magnetic field at 5.2 mm magnetic gap.

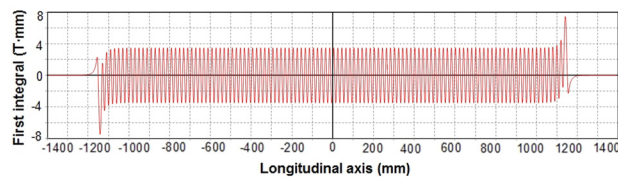


Figure 4: First field integral for the model at 5.2 mm gap.

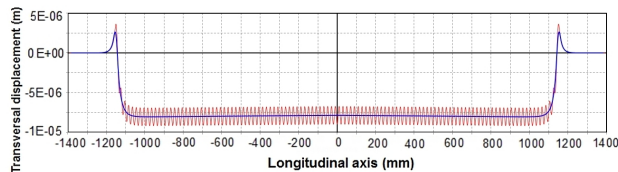


Figure 5: Transversal electrons excursion at 5.2 mm gap.

Demagnetizing Fields

Demagnetizing field in XZ plane is lower than 1.2 T ($\sim 1228 \text{ kA/m}$) and it is concentrated on the surface (Fig. 6). In XY plane it is below 1.54 T, as shown in Fig. 7.

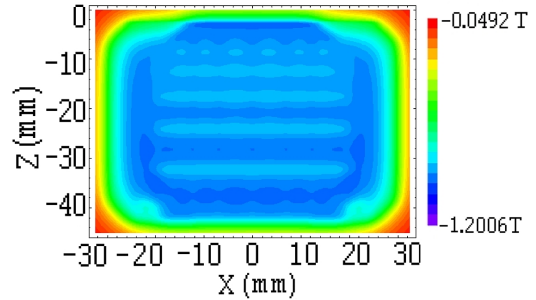


Figure 6: Demagnetizing field on the XZ surface of the magnet. Fields are always lower than 1.2 T.

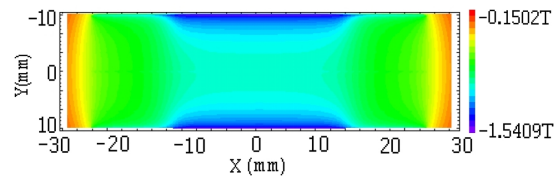


Figure 7: Demagnetizing field on the XY surface of the magnet block. Fields are always lower than 1.54 T.

EMISSION SPECTRUM

Spectrum at minimum gap, as well as the theoretical tuning curve, has been computed assuming 100 mA in the Storage Ring, using SPECTRA.[3] Results are shown in Figs. 8 and 9. The energy reached with 3rd harmonic is $< 4 \text{ keV}$ and Se K edge (12.6 keV) is reached with 9th harmonic with fair flux.

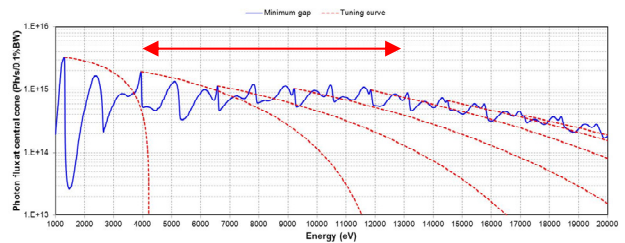


Figure 8: Spectral flux (Ph/s/0.1%BW) at 5.2 mm gap (blue) and tuning curves (red). Flux is continuous from 4 to 20 keV. Red arrows mark the useful range (4 – 13 keV).

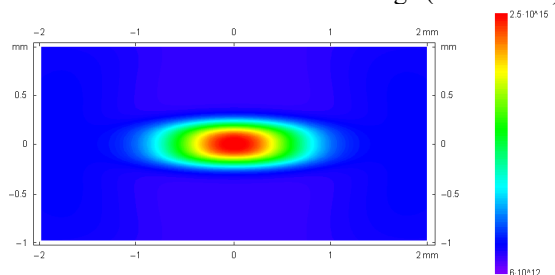


Figure 9: Flux density for 3rd harmonic (3.9 keV) at 10 m. Maximum flux is $2.5 \cdot 10^{15} \text{ Ph/s/mm}^2/0.1\% \text{BW}$.

Content from this work may be used under the terms of the CC BY 3.0 licence (© 2019). Any distribution of this work must maintain attribution to the author(s), title of the work, publisher, and DOI

This is a preprint — the final version is published with IOP

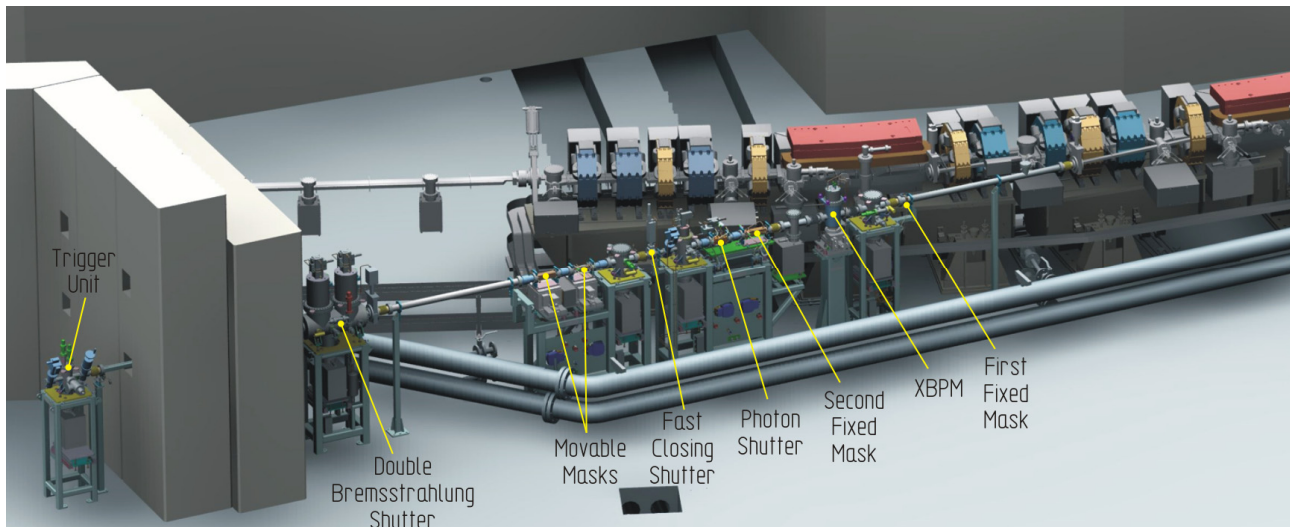


Figure 10: Layout of the XAIRA FE, integrated in the Storage Ring.

FRONT END

For the structure of the Front End (FE) the standard configuration used at existing ALBA beamlines [4] has been adopted. The design includes a couple of fixed masks, a photon beam position monitor (XBPM), a photon shutter, a double Bremsstrahlung shutter, a fast closing valve triggered by gauges installed on the BL side for protection of the accelerator's vacuum, and a set of moveable masks defining the photon beam size delivered to the users. The layout of the FE is shown in Fig. 10. All power absorbing elements have been dimensioned to withstand the beam delivered by a stored electron beam of up to 400mA.

Taking the design of BL13-XALOC FE as a starting point, we have adapted it to the enhanced power (6.9kW instead of 2.92kW) and on-axis power density (45.9kW/mrad² instead of 25.2kW/mrad²) delivered by XAIRA undulator. As a result it has been necessary to double the length of the second fixed mask (from 150mm up to 300mm) and to increase that of the movable masks by a 25% (from 200mm up to 250mm). In the same way as for BL13-XALOC FE, the body of those absorbers interacting with the undulator beam (second fixed mask, photon shutter and movable masks) will be made out of Glidcop® in order to cope with the large temperature gradients and mechanical stresses induced by it.

Given that the power delivered to the beamline optics shall always be kept below 1.3kW, an additional set of switches limiting the maximum angular aperture defined by the pair of movable masks has been incorporated into the design. The setting of these switches will be adjusted depending on the operating current of the Storage Ring in top-up mode: for stored currents not exceeding 250mA a maximum acceptance of 0.35×0.15mrad² will be established, whilst for currents up to 400mA it will be reduced down to 0.3×0.1mrad².

The FE is currently being manufactured by company FMB GmbH (Berlin, Germany), and it is expected to be delivered on October 2019.

CONCLUSION

The magnetic period and length of the designed photon source covers the range 4 - 20 keV photon energies with optimized photon flux without cryogenics.

The proposed insertion device fulfills therefore the two scientific aim of the beamline, namely, providing maximized flux at 12 KeV photon energy for micro-MX experiments and an energy range down to 4 keV.

Thanks to this, the phase determination using the anomalous signal of low-Z elements (S, Cl, K, Ca) naturally present in proteins is feasible.

Despite the considerable larger total power (×2.4) and maximum power density (×1.8) delivered by this photon source compared to existing IVUs at ALBA, we have been able to adapt our standard FE for IVU sources with only some minor modifications affecting the length of the critical power absorbing elements.

REFERENCES

- [1] Judith Juanhuix, Nahikari González, Damià Garriga, Josep Campmany, Jordi Marcos, Liudmila Nikitina, Carles Colldelram and Josep Nicolas, "Optical Design of the New Microfocus Beamline BL06-XAIRA at ALBA", AIP Conference Proceedings 2054, 060032 (2019). <https://aip.scitation.org/doi/10.1063/1.5084663>
- [2] P. Elleaume, O. Chubar, and J. Chavanne, "Computing 3D Magnetic Fields from Insertion Devices", in Proc. 17th Particle Accelerator Conf. (PAC'97), Vancouver, Canada, May 1997, paper 9P027, pp. 3509-3511.
- [3] Takashi Tanaka, "SPECTRA: a synchrotron radiation calculation code", *J. Synchrotron Rad.* (2001). 8, 1221-1228. <https://doi.org/10.1107/S090904950101425X>
Spectra homepage: <http://spectrax.org/spectra/>
- [4] J. Marcos, J. Campmany, D. Einfeld, and J. Pasquaud, "Front Ends at ALBA", in Proc. 2nd Int. Particle Accelerator Conf. (IPAC'11), San Sebastian, Spain, Sep. 2011, paper THPC055, pp. 3017-3019.